Corrosion protection of aluminium-matrix aluminium nitride and silicon carbide composites by anodization

JIANGYUAN HOU, D. D. L. CHUNG
Composite Materials Research Laboratory, State University of New York at Buffalo, Buffalo, NY 14260-4400, USA

Anodization is an effective surface treatment for improving the corrosion resistance of aluminium-matrix composites. For SiC particle-filled aluminium, anodization was performed successfully in an acid electrolyte, as usual. However, for AlN particle-filled aluminium, anodization needed to be performed in an akaline (0.7 N NaOH) electrolyte instead of an acid electrolyte, because NaOH reduced the reaction between AlN and water, whereas an acid enhanced this reaction. The concentration of NaOH in the electrolyte was critical; too high a concentration of NaOH caused the dissolution of the anodizing product (Al_2O_3) by the NaOH, whereas too low a concentration of NaOH did not provide sufficient ions for the electrochemical process. The corrosion properties and anodization characteristic of pure aluminium, Al/AlN and Al/SiC were compared. Without anodization, pure aluminium had better corrosion resistance than the composites and Al/SiC had better corrosion resistance than Al/AlN. After anodization, the corrosion resistance of Al/AlN was better than Al/SiC and both composites were better than pure aluminium without anodization, but still not as good as the anodized pure aluminium.

1. Introduction

Metal-matrix composites (MMCs) fabricated with lightweight aluminium alloy matrices and high-modulus SiC or AlN particle reinforcements, offer a low coefficient of thermal expansion and excellent mechanical properties. SiC-reinforced MMC is more commonly used than AlN-reinforced MMC, but AlN-reinforced MMC exhibits higher tensile strength and ductility at 300–400 °C and at room temperature after heating at 600 °C for 10–20 days. The latter also exhibits greater resistance to compressive deformation at 525 °C owing to the lack of a reaction between aluminium and AlN, in contrast to the reaction between aluminium and SiC in SiC-reinforced MMC [1]. Although both MMCs are promising for applications, the addition of a second phase to a metal matrix could significantly degrade the corrosion resistance.

Corrosion is usually prevented by chemical passivation coatings [2], polymer coatings [3] and/or anodized coatings [4]. The anodization of an aluminium alloy is an electrochemical method of converting aluminium to aluminium oxide (Al_2O_3) by applying an external current in the presence of an electrolyte. The most widely used electrolyte for anodizing is an acid, such as a sulphuric acid solution. There are two types of sulphuric acid anodizing: (1) conventional anodizing, which is performed at room temperature and provides a fairly hard oxide film about 10 μm thick; (2) hard anodizing, which is performed at 0 °C and provides a hard oxide film about 50 μm thick. The structure of the porous anodization layer was charactrized by Keller *et al.* [5] as a close-packed array of columnar hexagonal cells such that each cell contains a central columnar pore normal to the substrate surface. The porous layer has to be sealed in order to improve the corrosion resistance after anodizing. Through sealing, anodic coatings are partly converted to more voluminous boehmite ($Al_2O_3 \cdot nH_2O$), which plugs the pores [6].

The conventional anodizing method is less effective for the corrosion protection of aluminium MMCs than for aluminium alloys, owing to the presence of the reinforcement phase, which hinders the initiation and growth of the oxide film [7, 8]. The hard anodization method is usually used for high foreign-content alloys and MMCs. Several works [3, 7–12] have been reported on the effect of anodization on SiC-reinforced aluminium, but all of them are restricted to acid anodizing. It is commonly concluded that anodizing improves the corrosion resistance of all kinds of SiC-reinforced aluminium, though the effectiveness depends on the alloy used as the matrix. For example [11], the corrosion potential (higher for better corrosion resistance) of pure aluminium, aluminium alloy 6061 and their corresponding MMCs, was increased by about 140 mV for samples with a hard coating; hard anodizing did not improve the corrosion resistance of the 2024 Al alloy, but increased the corrosion potential of the MMC by up to 200 mV. In addition to the similar conclusion drawn regarding the effect of sulphuric acid anodizing on a SiC-reinforced aluminium, it is reported in the present work that sulphuric acid anodization shows little, if any, effect on AlN-reinforced pure aluminium. Anodizing in an alkaline

0022–2461

solution was used in this work to solve this problem. AlN-reinforced aluminium anodized in 0.7 N NaOH solution showed good corrosion resistance. Although there has been some work done on alkaline solution anodizing of metals, like iron or copper [13], no report has yet been made on aluminium anodizing in an alkaline solution.

Corrosion testing and monitoring are important elements of an overall programme to control corrosion. Various techniques have been used to evaluate the corrosion resistance. These include a salt-spray test as well as measurements of reflectivity, abrasion resistance and electrical breakdown voltage [7]. Electrochemical test methods are extremely useful in understanding and controlling corrosion, because they relate to the thermodynamics and kinetics of corrosion reactions; the electrochemical potential is equivalent to the driving force for the reaction; the current is equivalent to the reaction rate. The anodic polarization tests were used in the current work to study the corrosion properties of aluminium and aluminium-matrix composites.

2. Experimental procedure

Three kinds of materials were used, namely (1) pure aluminium (170.1), with composition 99.77% Al, 0.16% Fe and 0.07% Si, as supplied by Roth Brothers Smelting Corp., (2) pure aluminium matrix with 59 vol% AlN particle (Advanced Refractory Technologies Inc., Buffalo, NY, AlNel grade A-100) reinforcement (Al/AlN), and (3) pure aluminium matrix with 58 vol% SiC particle (Electro Abrasives Corp., Lackawana, NY, 1200-W) reinforcement (Al/SiC).

The AlN particle size ranged from 2–7 μm, with a mean of 3.7 μm. The composition of AlN was 66.0% Al, 33.0% N, 0.07% C, 1.0% O, 0.005% Fe and 0.005% Si. The SiC particle size ranged from 1 to 10 μm, with a mean of 3 μm. The composition of SiC was 98.5% SiC, 0.5% SiO_2, 0.3% Si, 0.08% Fe, 0.1% Al, 0.3% C.

AlN and SiC composites were fabricated by liquid-metal infiltration [15], with argon (UN1600) as the pressurizing gas. The AlN-reinforcement preform was baked at 200 °C for 8 h and then furnace cooled. The SiC-reinforcement preform was baked at 550 °C for 2 h and then furnace cooled.

All the materials were anodized in an electrolyte at 0 °C, with a pure aluminium plate as the cathode. Pure aluminium was etched in 10% NaOH solution at 40 °C, electrochemically polished in 50% HNO_3 solution at room temperature and then anodized in 10 vol% H_2SO_4 for 0.5 h. Al/AlN and Al/SiC were ground to 600 grit, mechanically polished and then rinsed in water and methanol before anodization in both 10 vol% H_2SO_4 and 0.7 N NaOH (as electrolytes) for 1 h. The composites were not etched, because there was negligible native oxide film on the surface of composites compared to that on the surface of pure aluminium. Additionally, the high reinforcement content of the composite surface made etching very preferential, and there was essentially no aluminium left on the composite surface after etching, as shown by scanning electron microscopy (SEM). Anodization applied on the etched Al/AlN and Al/SiC did not result in an anodization film.

The current density in the anodization process was controlled at 25 mA mm^{-2} by a Harrison 6294A d.c. power supply; the voltage during anodization was measured by a Harrison DM350 potential meter. Pure aluminium and the Al/SiC composite were sealed in distilled water at 90–100 °C for 30 min after anodization. The corrosion potential of 10 vol% H_2SO_4 anodized Al/AlN without sealing was − 660 mV, and that with sealing was − 670 mV; in contrast, the corrosion potential of 10 vol% H_2SO_4 anodized Al/SiC without sealing was − 590 mV, and that with sealing was − 510 mV [16]. Because sealing had no positive effect on anodized Al/AlN, no sealing was applied to Al/AlN after anodization. However, sealing was applied to Al/SiC after anodization.

Electrochemical polarization resistance measurement and potentiodynamic scan testing were used to study the corrosion properties of aluminium and aluminium-matrix composites in 0.5 N NaCl (open to the air). The instrument used was the CMS105 d.c. corrosion test system of Gamry Instruments, Inc. (Willow Grove, PA). A saturated calomel electrode (SCE) was used as the reference electrode and a platinum wire was used as the counter electrode.

The corrosion current is the current when the tested sample is in a freely corroding open-circuit condition, in which there is no net transfer of charge. The corrosion potential is the open-circuit potential. In the polarization experiment, the potential was scanned from 20 mV below the corrosion potential to 20 mV over the corrosion potential. As the same time, the current flowing from the test sample to the counter electrode was measured.

Anodic polarization experiments were started after a steady open-circuit potential (corrosion potential) was achieved. The scan rate for the polarization resistance test was 5 mV s^{-1}. Over the scan range of the polarization resistance test, the current versus voltage curve was roughly linear. An applied potential that is more positive than the corrosion potential results in an anodic current, whereas a potential that is more negative than the corrosion potential results in a cathodic current. A linear fit of the data to a standard model yields an estimate of the polarization resistance, R_p, which describes the corrosion resistance of the sample tested. The higher is the R_p, the better is the corrosion resistance. The relationship of R_p to the corrosion current density (corrosion current divided by the exposed area), i_{corr}, is

$$R_p = \beta_a\beta_c/2.3i_{corr}(\beta_a + \beta_c) \quad (1)$$

where β_a and β_c are the Tafel slopes for the anodic and cathodic regimes, which are constant for any fixed system. The values of β_a and β_c are either determined experimentally or estimated. In the present work, β_a and β_c are both estimated to be 0.12 V per decade (i.e. the change in potential is equal to 0.12 V for each ten-fold change in current), based on the typical Tafel curve of the MMC (Fig. 1). Each value of corrosion current density and polarization resistance listed in

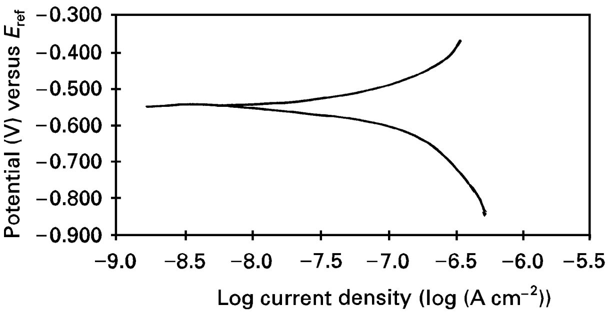

Figure 1 Typical Tafel curve for MMC.

TABLE I Corrosion properties of aluminium and its composites

	Corrosion potential (mV ± 5 mV)	Corrosion current density (A cm^{-2})	Polarization resistance (Ω cm^2)
Pure Al	− 760	$2.4 \times 10^{-8} \pm 5 \times 10^{-9}$	$1.1 \times 10^6 \pm 5 \times 10^5$
Al/AlN	− 680	$1.4 \times 10^{-6} \pm 5 \times 10^{-7}$	$3.5 \times 10^4 \pm 5 \times 10^3$
Al/SiC	− 610	$1.2 \times 10^{-6} \pm 5 \times 10^{-7}$	$5.7 \times 10^4 \pm 5 \times 10^3$

Tables I and III–V (see later) is the average of at least three test results.

The anodic polarization diagrams (potentiodynamic test) of all the materials were generated to identify the corrosion mechanisms. All the potentiodynamic tests were run at a scan rate of 0.15 mV s^{-1}, from 200 mV below the corrosion potential to 1.5 V.

The volume resistivity of each composite was measured by using the four-probe method. Silver paint electrical contacts were applied circumferentially in four planes perpendicular to the current direction in order to form the four probes. A Keithley 2001 multimeter was used.

The capacitance of the differnt kinds of anodized film was measured by using a QuadTech Model 7600 RLC Meter at a frequency of 1000 Hz. The anodized film on one side of an anodized sample was removed by polishing. An electric field was applied perpendicular to the film through two copper cylinders, which were pressed firmly during the test to sandwich the sample and function as pressure electrical contacts. The capacitance of the anodized film, with a copper pressure contact on one side and the substrate (Al, Al/SiC or Al/AlN) on the other side, was measured. The relative dielectric constant was calculated from the measured capacitance.

The exposed surfaces after each kind of experiment were examined with an optical microscope and an SEM to characterize the corrosion morphology.

3. Results and discussion

Table I shows the results of the polarization resistance measurement of pure aluminium, Al/AlN and Al/SiC without any surface treatment. The corrosion current density of pure aluminium was lower than those of both Al/AlN and Al/SiC. This is because the high volume fraction of either reinforcement degraded the uniformity of the natural oxide film on the surface and thus decreased the corrosion resistance of the composites. Because both AlN and SiC are not electrically conductive materials, the corrosion potential of the two composites were less negative than pure aluminium, even though the corrosion rates (corrosion current densities) of the composites were higher than that of pure aluminium.

Comparison of the corrosion potential, corrosion current density and polarization resistance of Al/AlN and Al/SiC shows that the corrosion resistance of Al/SiC was a little better than that of Al/AlN. The electrical resistivity, ρ, of Al/AlN was a little lower than that of Al/SiC: $\rho_{Al/AlN} = (1.8 \pm 0.05) \times 10^{-4}$ Ωcm, $\rho_{Al/SiC} = (2.2 \pm 0.05) \times 10^{-4}$ Ω cm. However, the electrical resistivity difference was small, so it is not the main cause of the difference in corrosion resistance between the two composites. The main reason that Al/SiC exhibited better corrosion resistance than Al/AlN is that the AlN reinforcement reacts with water, according to Equation 2, while SiC does not

$$AlN + 3H_2O = Al(OH)_3 + NH_3 \qquad (2)$$

The corrosion resistance of Al/SiC is better than that of Al/AlN when no surface treatment is involved.

Figs 2–4 show the potentiodynamic curves of pure aluminium, Al/AlN and Al/SiC (both composites without anodization), respectively. Corrosion started at a lower current density for pure aluminium (10^{-7} A cm^{-2}) than for Al/AlN and Al/SiC (10^{-6} A cm^{-2}). Moreover, the corrosion current density increased with increasing potential less rapidly for pure aluminium than for the two composites. The curves for Al/AlN and Al/SiC composites were essentially the same.

Table II shows the corrosion potential of Al/AlN anodized in NaOH at different concentrations. By

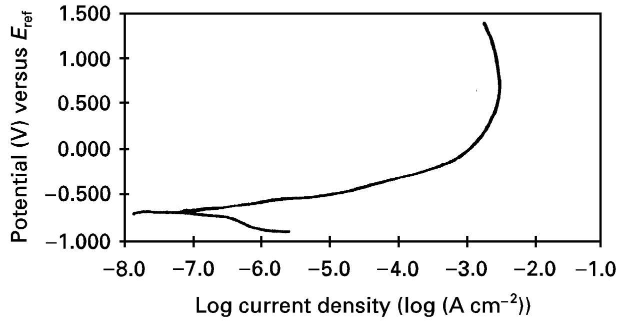

Figure 2 Potentiodynamic curve of pure aluminium.

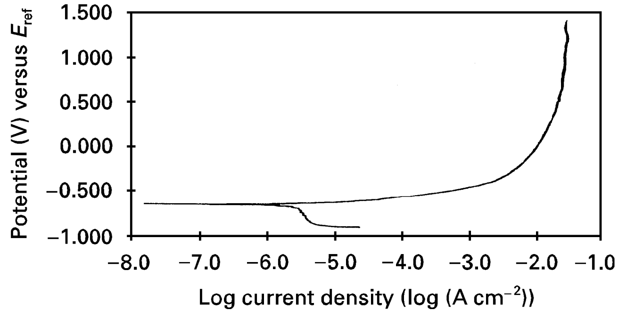

Figure 3 Potentiodynamic curve of Al/AlN without anodization.

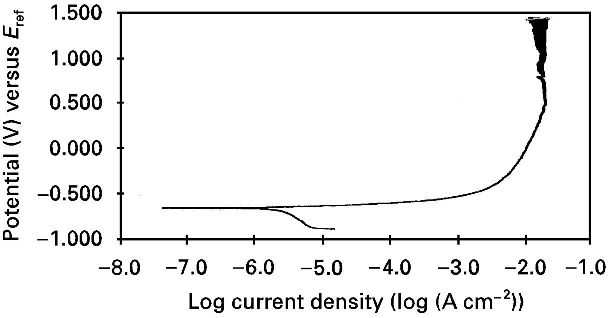

Figure 4 Potentiodynamic curve of Al/SiC without anodization.

TABLE II Corrosion potential of Al/AlN under different conditions

Al/AlN	Corrosion potential (mV ± 5 mV)
Without anodization	− 680
Anodized in 0.3 N NaOH at 0 °C	− 690
Anodized in 0.7 N NaOH at 0 °C	− 440
Anodized in 1.0 N NaOH at 0 °C	− 700

anodizing in an NaOH solution with an appropriate NaOH concentration, the corrosion resistance was improved greatly. However, the concentration of NaOH was critical; only the concentration of 0.7 N gave a less negative corrosion potential (i.e. better corrosion resistance) than the case without anodization. Concentrations of 0.9 and 0.3 N did not give any satisfactory result. The principal electrochemical reactions occurring during the anodization of Al/AlN in NaOH are believed to be the following

$$Al = Al^{3+} + 3e^- \quad (3)$$

$$2Al^{3+} + 3H_2O = Al_2O_3 + 6H^+ \quad (4)$$

$$O_2 + 2H_2O + 4e^- = 4OH^- \quad (5)$$

where the OH^- ions provided by NaOH reduced the reaction between AlN and water (Equation 2) and thus enhanced the growth rate of the Al_2O_3 film. If the concentration of the NaOH is too low, the NaOH will not be effective, because there are not enough OH^- ions to reduce the reaction between AlN and water (Equation 2). Too high a concentration of NaOH is not effective for enhancing the growth rate of the oxide film either, because NaOH at a high enough concentration dissolves Al_2O_3 and aluminium.

Fig. 5 is the curve of voltage versus time during the anodization of Al/AlN at 0 °C in NaOH at different concentrations. The voltage remained at around 30 V during the whole anodization process in 0.3 N NaOH solution. This means that there was no oxide film formed at all. In a 0.9 N NaOH solution, the voltage increased and then decreased in an oscillating fashion during anodization. This means that the anodized film was dissolved immediately after it formed. Only the curve for anodizing in 0.7 N NaOH turned out to be a stable line at 60 V, implying stable growth of the anodization film. This result is consistent with the corrosion potentials in Table II.

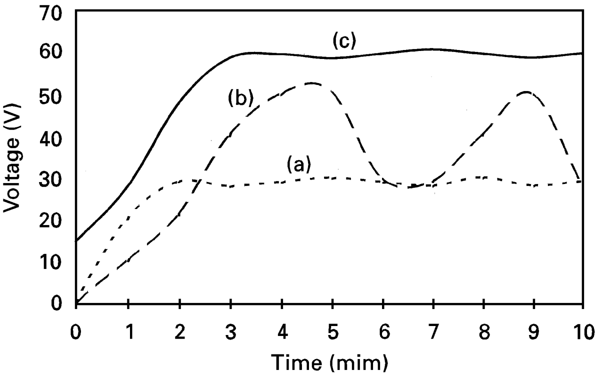

Figure 5 Voltage verse time curves during the anodization of Al/AlN in NaOH, anodized in (a) 0.3 N, (b) 0.9 N and (c) 0.7 N NaOH.

Table III shows the corrosion properties of Al/AlN under different conditions. Acid anodization (10 vol% H_2SO_4) hardly had any effect on the corrosion resistance of the composite, but alkaline anodization (0.7 N NaOH) grately improved the corrosion resistance of Al/AlN. After the NaOH anodization, the corrosion potential increased by 240 mV, the corrosion current decreased from 1.4×10^{-6} to 3.0×10^{-10} A cm^{-2}, while the polarization resistance increased from 3.5×10^4 to 1.4×10^8 Ω cm^{-2}. Because an acid solution enhanced the reaction between water and AlN (Equation 2) in the anodizing process, it was difficult to obtain a uniform and continuous film by acid anodization of Al/AlN. By anodizing Al/AlN in NaOH, the corrosion resistance was improved greatly. This is because NaOH greatly reduced the reaction between water and AlN, so that a more compact and continuous coating was formed. It should be noted that $Al(OH)_3$ formed by Equation 2 is equivalent to $Al_2O_3 \cdot nH_2O$, which is akin to the anodized film itself, thereby enhancing the smoothness of the anodized film. The film microstructure is described later in this section.

Figs 3, 6 and 7 show the potentiodynamic curves of Al/AlN under different conditions. Figs 3 and 6 show that the polarization behaviour of Al/AlN without anodization and that after acid anodization are similar. Fig. 7 shows that, after alkaline anodization, corrosion starts at a lower current density (10^{-10} A cm^{-2}) and a less negative corrosion potential, and the corrosion current density increases with the potential less rapidly.

Table IV shows the corrosion properties of Al/SiC at different conditions of anodization. Alkaline anodization had little effect on the corrosion resistance of Al/SiC, because the positive effect of NaOH mentioned above for Al/AlN is not applicable to Al/SiC. Because the interface between SiC and pure aluminium is not as good as that between AlN and pure aluminium, Al/AlN was a better composite for anodization. Owing to the poor interface between SiC particles and the anodization film, the anodized film had to grow around the SiC particles, leaving small gaps between SiC particles and anodized film both around and above the particles. The effect of a poor interface was particularly significant in the case of alkaline

TABLE III Corrosion properties of Al/AlN

Al/AlN	Corrosion potential (mV ± 5 mV)	Corrosion current density ($\mathrm{A\,cm^{-2}}$)	Polarization resistance ($\Omega\,\mathrm{cm}^2$)
Without anodization	− 680	$1.4 \times 10^{-6} \pm 5 \times 10^{-7}$	$3.5 \times 10^4 \pm 5 \times 10^3$
H_2SO_4 anodized	− 540	$1.0 \times 10^{-6} \pm 5 \times 10^{-7}$	$5.4 \times 10^5 \pm 5 \times 10^4$
NaOH anodized	− 440	$3.0 \times 10^{-10} \pm 5 \times 10^{-11}$	$1.4 \times 10^8 \pm 5 \times 10^7$

TABLE IV Corrosion properties of Al/SiC

Al/SiC	Corrosion potential (mV ± 5 mV)	Corrosion current density ($\mathrm{A\,cm^{-2}}$)	Polarization resistance ($\Omega\,\mathrm{cm}^2$)
Without anodization	− 610	$1.2 \times 10^{-6} \pm 5 \times 10^{-7}$	$5.7 \times 10^4 \pm 5 \times 10^3$
H_2SO_4 anodized	− 510	$1.4 \times 10^{-9} \pm 5 \times 10^{-10}$	$6.8 \times 10^7 \pm 5 \times 10^6$
NaOH anodized	− 680	$4.5 \times 10^{-7} \pm 5 \times 10^{-8}$	$5.9 \times 10^4 \pm 5 \times 10^3$

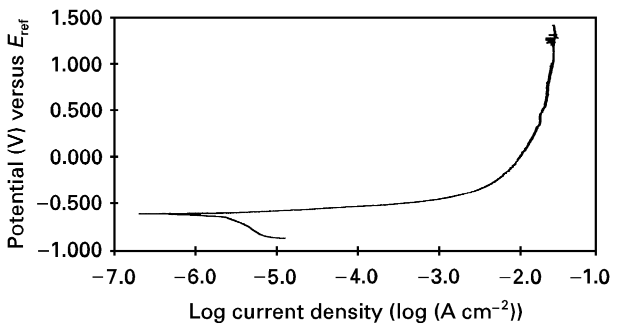

Figure 6 Potentiodynamic curve of Al/AlN anodized in H_2SO_4 solution.

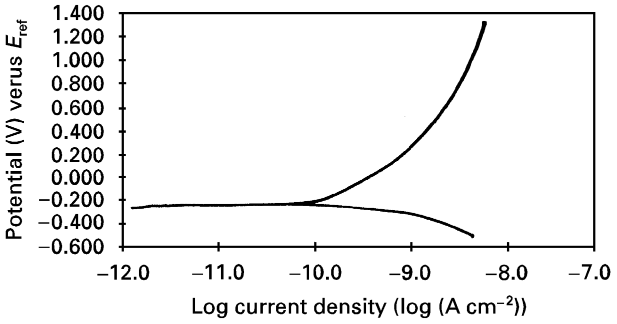

Figure 7 Potentiodynamic curve of Al/AlN anodized in NaOH solution.

anodization, as the film growth rate was much lower and the resulting film was thinner for alkaline anodization than acid anodization. However, acid anodization decreased the corrosion current density of Al/SiC from $1.2 \times 10^{-6}\ \mathrm{A\,cm^{-2}}$ to $1.4 \times 10^{-9}\ \mathrm{A\,cm^{-2}}$ and the polarization resistance was increased from 5.7×10^4 to $6.8 \times 10^7\ \Omega\,\mathrm{cm}^2$. The corrosion potential of Al/SiC was also increased by 100 mV by acid anodization. The incompatible interface problem still existed in acid anodization, but was not as dominating as in NaOH solution anodization, because the film growth was much more rapid, and the ultimate film thickness was larger for a film anodized in an acid solution than that anodized in an alkaline solution. Therefore, acid anodization plus sealing still improved the corrosion resistance of Al/SiC, whereas alkaline anodization had little effect.

Figs 4, 8 and 9 show the potentiodynamic curves of Al/SiC under different conditions. The important characteristic of the potentiodynamic curves for Al/SiC without anodization and that after NaOH anodization are about the same, while the potentiodynamic curve of Al/SiC after acid anodization started at a lower corrosion current density and propagated at a lower rate. The electrochemical reactions during the acid anodization of Al/SiC have been summarized by Tajima [6]

$$\mathrm{Al} = \mathrm{Al}^{3+} + 3\mathrm{e}^- \qquad (6)$$

$$2\mathrm{Al}^{3+} + 3\mathrm{H_2O} = \mathrm{Al_2O_3} + 6\mathrm{H}^+ \qquad (7)$$

$$\mathrm{SO_4^{2-}} = \mathrm{SO_3} + \mathrm{O}^{2-} \qquad (8)$$

$$2\mathrm{Al}^{3+} + 3\mathrm{O}^{2-} = \mathrm{Al_2O_3} \qquad (9)$$

Table V shows the corrosion properties of pure aluminium with and without anodization. Acid anodization decreased the corrosion current density of pure aluminium from $2.4 \times 10^{-8}\ \mathrm{A\,cm^{-2}}$ to $2.5 \times 10^{-12}\ \mathrm{A\,cm^{-2}}$. The polarization resistance was increased from $1.1 \times 10^6\ \Omega\,\mathrm{cm}^2$ to $6.8 \times 10^{10}\ \Omega\,\mathrm{cm}^2$. The corrosion potential of pure aluminium was increased by 360 mV by anodization. Figs 2 and 10 show the potentiodynamic curves of pure aluminium without and with anodization, respectively. Anodization shifted the curve to a much lower current density and slower rate of current density increase.

Comparison of Tables II, III and IV shows that pure aluminium after anodization had the best corrosion resistance. This is due to the superior quality of the anodization film on pure aluminium compared to that of the anodization film in Al/AlN or Al/SiC. Fig. 11 shows the cross-sectional view of the anodization (with appropriate electrolyte) films on pure aluminium, Al/AlN and Al/SiC. Pure aluminium had the most uniform and compact coating and the coating was continuous, with a thickness of 30 μm. The coatings on

TABLE V Corrosion properties of pure aluminium

	Corrosion potential (mV ± 5 mV)	Corrosion current density (A cm^{-2})	Polarization resistance (Ω cm^2)
Without anodization	− 760	$2.4 \times 10^{-8} \pm 5 \times 10^{-9}$	$1.1 \times 10^{6} \pm 5 \times 10^{5}$
H_2SO_4 anodized	− 400	$2.5 \times 10^{-12} \pm 5 \times 10^{-13}$	$6.8 \times 10^{10} \pm 5 \times 10^{9}$

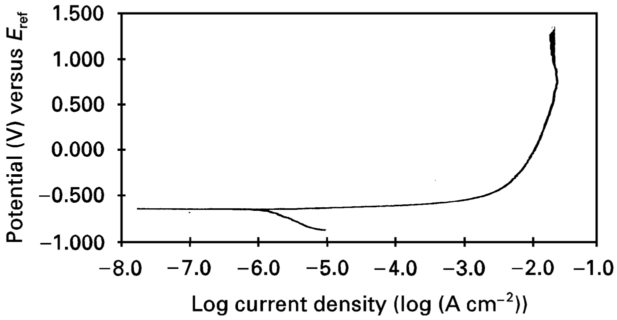

Figure 8 Potentiodynamic curve of Al/SiC anodized in NaOH solution.

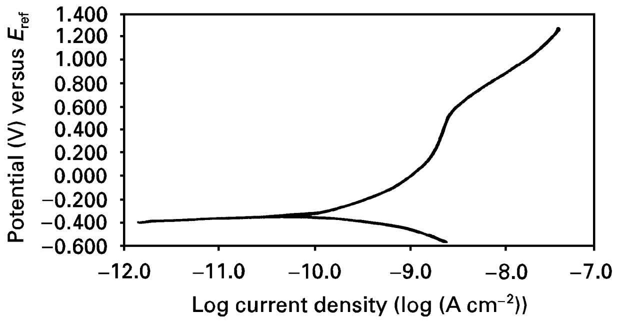

Figure 9 Potentiodynamic curve of Al/SiC anodized in H_2SO_4 solution.

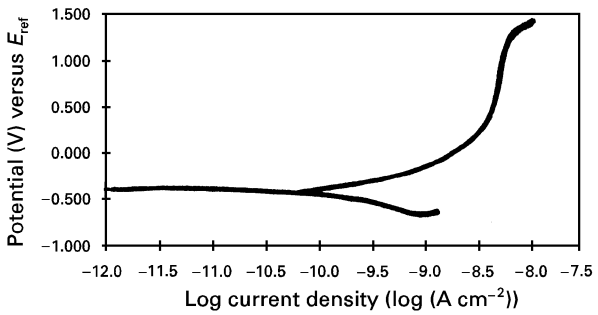

Figure 10 Potentiodynamic curve of pure aluminium anodized in H_2SO_4 solution.

Al/AlN and Al/SiC were not continuous or uniform. Fig. 12 is the plan view of the anodization coating on the three materials. The coating on pure aluminium had the smallest and fewest pores, while the coating on the Al/SiC had the most numerous and biggest pores. The presence of the SiC and AlN particulate inhibited the formation of a continuous barrier layer of the anodization film on the composites. As a result, the thickness of the anodization film could not be measured for the composites.

The corrosion resistance of Al/AlN was not as good as Al/SiC before anodization, but was better than Al/SiC after anodization with the appropriate electrolyte (alkaline for Al/AlN and acid for Al/SiC). This is

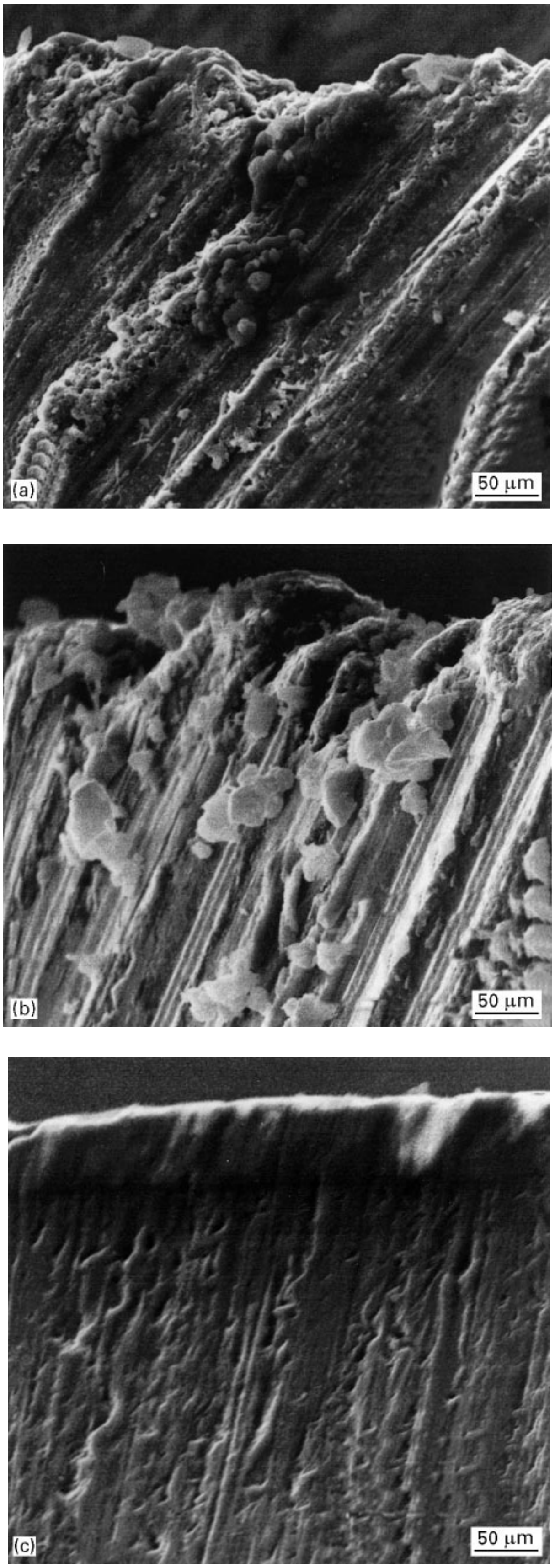

Figure 11 Cross-sectional view of the anodization films. (a) Al/AlN, (b) Al/SiC, (c) pure aluminium.

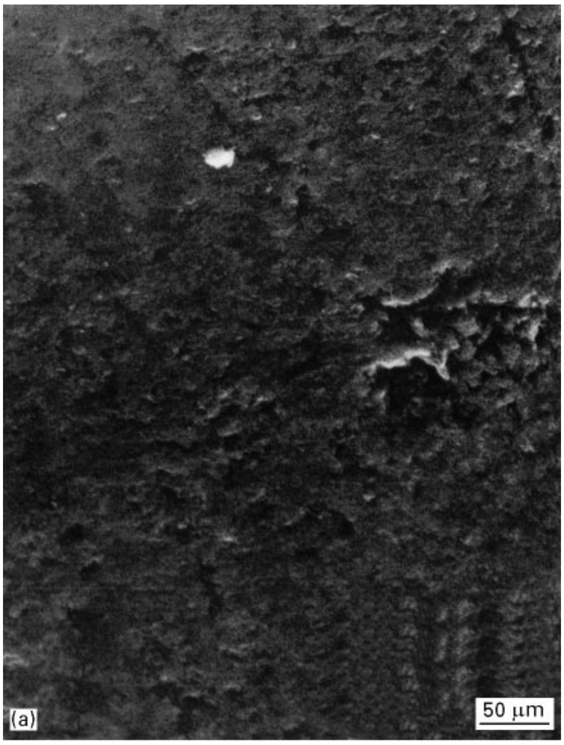

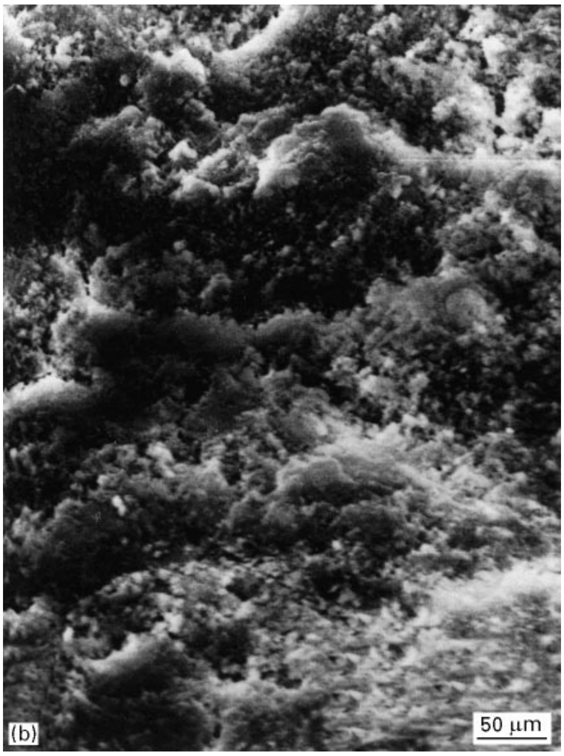

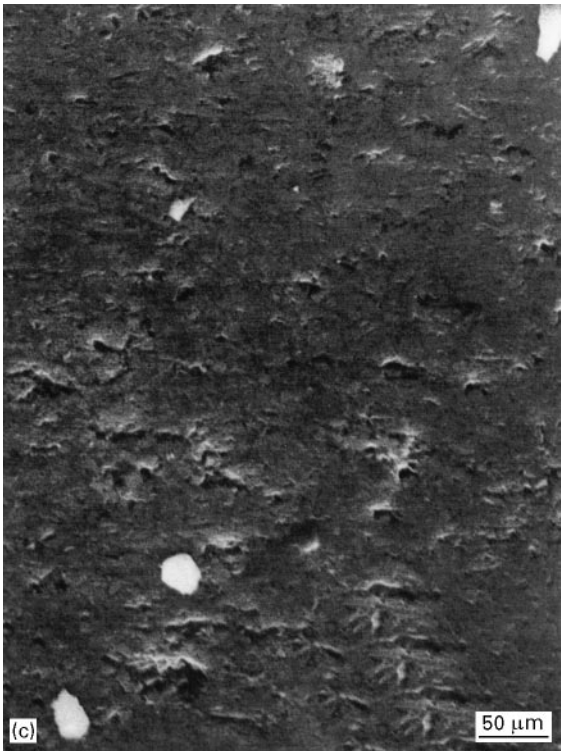

Figure 12 Plan view of the anodization films. (a) Al/AlN, (b) Al/SiC, (c) pure aluminium.

partly due to the difference in the anodization coating morphology between the two composites. Fig. 13 shows the surface morphology of the two composites (without anodization) after mechanical polishing. The Al/SiC had more pores on the polished surface than Al/AlN. Owing to the reaction between SiC and Al, i.e.

$$3SiC + 4Al = 3Si + Al_4C_3 \qquad (10)$$

a brittle reaction product (Al_4C_3) lined the interface between SiC and aluminium. This contributed to causing the removal of some SiC particles during polishing. Because every sample was polished before anodization, the original surface of Al/SiC was not as uniform as that of Al/AlN. Comparison of Fig. 12a and b shows that the anodization coating on Al/SiC was more porous than that on Al/AlN. The cross-sectional view (Fig. 11) also shows that the coating on Al/SiC was less compact than that on Al/AlN. The other reason that anodized Al/AlN exhibited better corrosion resistance than anodized Al/SiC is that Al/AlN was anodized in a low-concentration alkaline solution, whereas Al/SiC was anodized in an acid solution. The anodized film was almost insoluble in the alkaline solution and, because of the non-reactivity between the AlN particle and both the aluminium matrix and the Al_2O_3 film, an adherent film was formed on Al/AlN. The more continuous anodization film formed in this way was more corrosion resistant than the film formed by acid anodization.

Fig. 14 shows the surface morphology of all the samples after being polarized to 1.5 V during the potentiodynamic experiment. The morphology of corrosion (up to a potential of 1.5 V) of both Al/SiC and Al/AlN before and after anodization was the same. Al/SiC had bigger and deeper pits than Al/AlN, while pure aluminium without anodization had smaller and shallower pits than both composites. The anodized pure aluminium had bigger but fewer pits than all the other samples.

Values of the relative dielectric constant of different anodized films shown in Table VI support the above explanation. The anodization film on pure aluminium had the highest relative dielectric constant among the three kinds of anodization film. This suggests that this anodization film was the most compact film. The anodization film on Al/AlN had a relative dielectric constant slightly higher than that of the film on

Al/SiC, suggesting that the anodization film on Al/AlN was a little more compact than that on Al/SiC. For comparison, measurement of the relative dielectric constant was made on a sheet of Al_2O_3. The value obtained was 6.3. This high value suggests that all the anodization films were probably not pure Al_2O_3, but rather $Al_2O_3.nH_2O$, as porosity alone could not account for the low values for the anodization films.

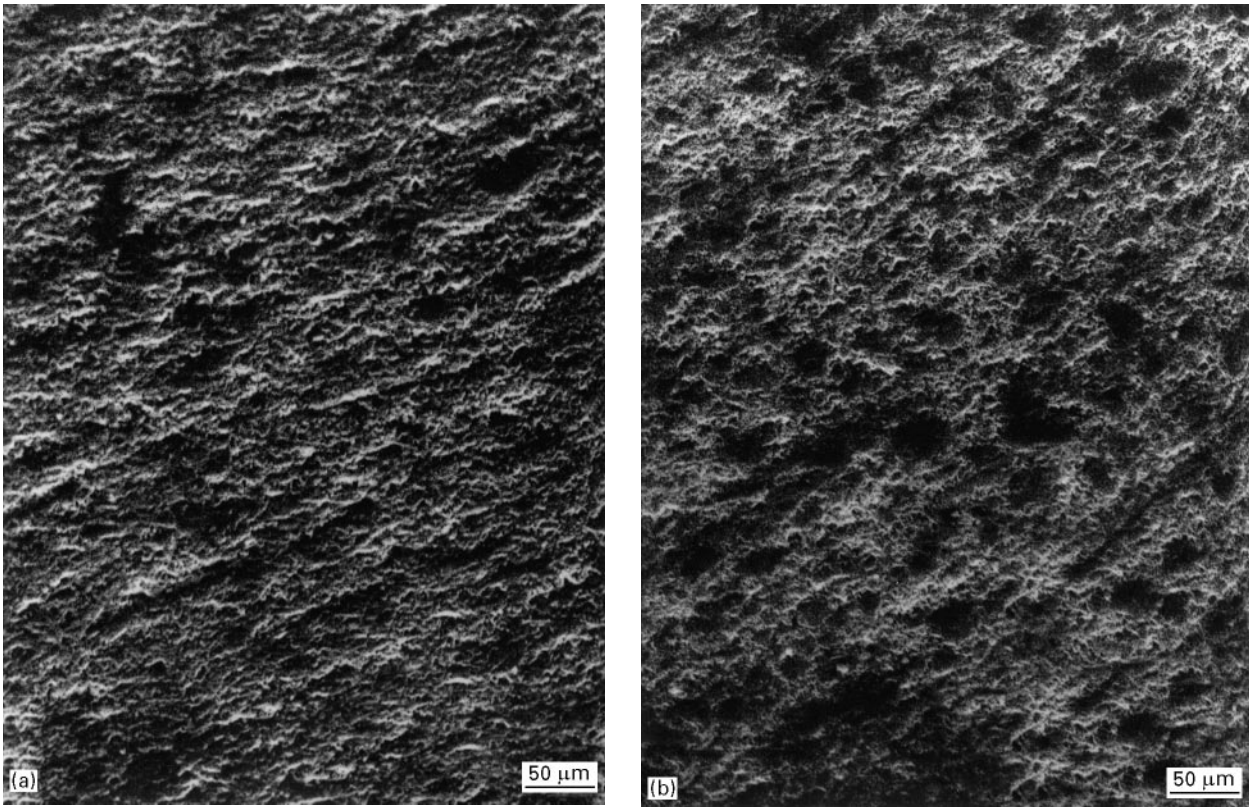

Figure 13 Surface morphology of (a) Al/AlN and (b) Al/SiC before anodization.

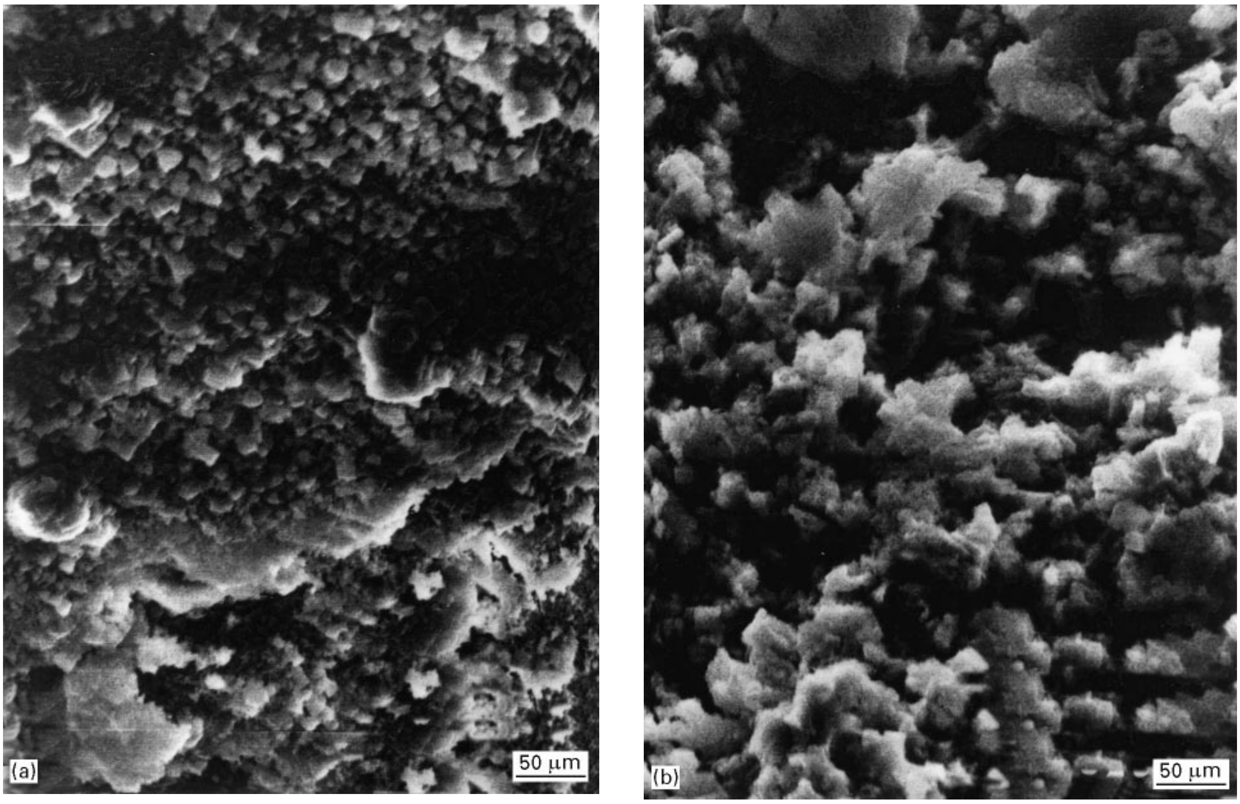

Figure 14 Continued

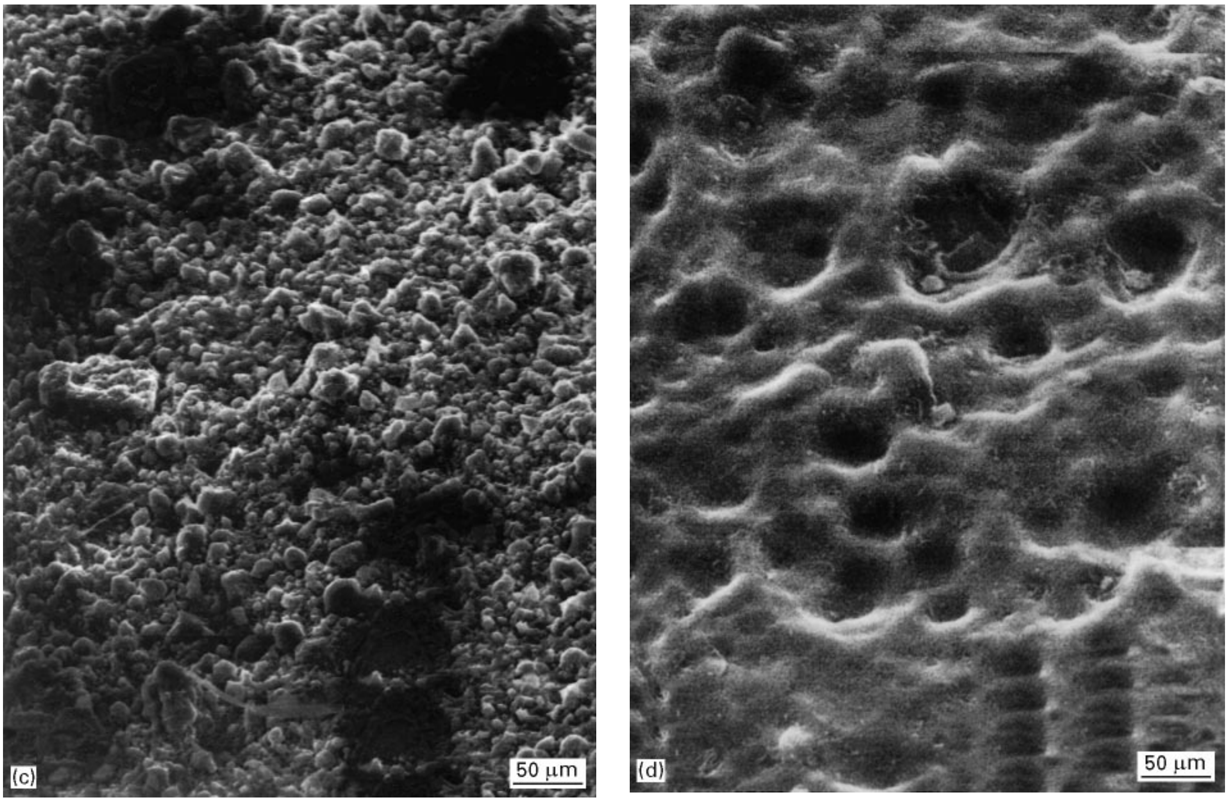

Figure 14 Surface morphology of Al/AlN, Al/SiC and pure aluminium after the potentiodynamic experiment: (a) Al/AlN, (b) Al/SiC, (c) pure aluminium (d) anodized pure aluminium; (a, b, c) without anodization.

TABLE VI Relative dielectric constant

	Relative dielectric constant
Anodized pure Al	2.4 ± 0.1
Anodized Al/SiC	1.2 ± 0.1
Anodized Al/AlN	1.4 ± 0.1

4. Conclusion

Without anodization, Al/AlN was less corrosion resistant than Al/SiC. Sulphuric acid hard anodization and subsequent sealing improved the corrosion resistance of Al/SiC, but they had negligible effect on Al/AlN. NaOH anodization at 0 °C improved the corrosion resistance of Al/AlN greatly when an appropriate NaOH concentration (0.7 N) was used. With appropriate anodization, Al/AlN was more corrosion resistant than Al/SiC. The anodization film on Al/AlN was more continuous and compact than that on Al/SiC, because AlN particles react with water to form $Al(OH)_3$, which is equivalent to $Al_2O_3 \cdot nH_2O$. Formation of $Al_2O_3.nH_2O$ enhances the growth of the anodization film. Without anodization, the corrosion resistance of Al/AlN and Al/SiC was not as good as that of pure aluminium, but appropriately anodized Al/AlN and Al/SiC had better corrosion resistance than pure aluminium without anodization. The anodized pure aluminium was more corrosion resistant than both Al/AlN and Al/SiC after appropriate anodization.

Acknowledgement

This work was supported in part by the Defence Advanced Research Projects Agency of the US Department of Defense.

References

1. SHY-WEN LAI and D. D. L. CHUNG, *J. Mater. Sci.* **29** (1994) 6181.
2. A. TURNBULL, NPL Report DMM (A) 15 (National Physical Laboratory, Teddington, Middlesex, UK, 1990).
3. S. LIN and H. GREENE, *Corrosion* **48** (1992) 61.
4. F. MANSFELD and S. LIN, *ibid.* **45** (1989) 615.
5. F. KELLER, M. S. HUNTER and O. L. ROBINSON, *J. Electrochem. Soc.* **100** (1983) 411.
6. S. TAJIMA, “Advances in Corrosion Science and Technology”, Vol. 1, (Plenum Press, New York, NY, 1970) p. 229.
7. P. P. TRZASKOMA and E. McCAFFERTY, in “Proceedings of the Symposium on Aluminum Surface Treatment Technology, ’86” edited by R. S Alwitt and G. E. Thompson (Electrochemical Society, Pennington, NJ, USA, 1986) p. 171.
8. F. MANSFELD and S. L. JEANJAQUET, *Int. Corros. Conf. Ser.* **NACE-9** (*Adv. Localized Corrs.*) (1990) 343.
9. P. P. TRZASKOMA, *Corrosion* (*Houston*) **46** (1990) 402.
10. E. McCAFFERTY and P. P. TRZASKOMA, *J. Electrochem. Soc.* **130** (1983) 1804.
11. E. McCAFFERTY and P. P. TRZASKOMA, *Int. Corros. Conf. Ser.* **NACE-9** (*Adv. Localized Corros.*) (1990) 181.
12. E. MANSFELD and S. L. JEANJAQUET, *Corrs. Sci.* **29** (1986) 727.
13. M. R. GENERRO DE CHIALVO and J. O. ZERBONI, *J. Appl. Electrochem.* **16** (1986) 517.
14. R. K. DHIR, M. R. JONES and M. J. McCARTHY, *Cem. Concr. Res.* **23** (1993) 1443.
15. JINGYU YANG and D. D. L. CHUNG, *J. Mater. Sci.* **24** (1989) 3605.
16. JIANGYUAN HOU and D. D. L. CHUNG, *Mater. Res. Soc. Symp. Proc.* **390** (*Electronic Packaging Materials Science VII*) (1995) 129.

Received 29 August
and accepted 30 October 1996